Order in Extremal Trajectories

**Khanh-Dang Nguyen Thu Lam · Jorge Kurchan ·
Dov Levine**

Abstract Given a chaotic dynamical system and a time interval in which some quantity takes an unusually large average value, what can we say of the trajectory that yields this deviation? As an example, we study the trajectories of the archetypical chaotic system, the baker's map. We show that, out of all irregular trajectories, a large-deviation requirement selects (isolated) orbits that are periodic or quasiperiodic. We discuss what the relevance of this calculation may be for dynamical systems and for glasses.

Keywords Amorphous solids · Chaos · Order

1 Introduction

In this paper we discuss, with the aid of a simple example, how order arises from chaos when we select the solutions that minimize some quantity. The motivation for this work is twofold, one related to dynamical systems, and the other to glasses.

Consider first a chaotic dynamical system, for example a liquid flowing past an obstacle, at large Reynolds numbers. The wake behind the obstacle is chaotic, and the pressure it creates may exhibit considerable fluctuations. We may ask the question: given that during a certain time-interval the average pressure has been abnormally large, what can we say about the velocity field during that time? Is it reasonable to assume that, if the high pressure is to last long, then the fluid phase-space trajectory has to have during that time some regularity that is absent in a typical chaotic trajectory? What we are asking, then, is a question on

K.-D. Nguyen Thu Lam
M2 SDSMC–PTSC, Université Paris VII, Paris, France

J. Kurchan (✉)
CNRS-ESPCI, rue Vauquelin 10, 75231 Paris, France
e-mail: jorge@pmmh.espci.fr

D. Levine
Department of Physics, Technion, Haifa 32000, Israel

the large deviation functions of a chaotic system: are the trajectories that sustain extreme situations special, and in a sense simpler?

A second motivation is related to the question of the nature of the order in an ideal, equilibrium, glass state—if, of course, such a thing exists. An approach to the glass problem [1–3] is to consider a free-energy density functional in d-dimensional space [4]:

$$F[\rho(\mathbf{x})] = \int d^d\mathbf{x} \, \rho[\ln\rho(\mathbf{x}) - 1] - \frac{1}{2}\int d^d\mathbf{x} \, d^d\mathbf{x}' \, [\rho(\mathbf{x}) - \rho_o]C(\mathbf{x} - \mathbf{x}')[\rho(\mathbf{x}') - \rho_o] \quad (1)$$

where $C(\mathbf{x} - \mathbf{x}', \rho_o)$ is the liquid direct correlation function at average density ρ_o. We look for the 'local' free energy minima that satisfy:

$$\frac{\delta F[\rho(\mathbf{x})]}{\delta\mathbf{x}} = \ln\rho(\mathbf{x}) - \int d^d\mathbf{x}' \, C(\mathbf{x} - \mathbf{x}', \rho_o)[\rho(\mathbf{x}') - \rho_o] = 0 \quad (2)$$

At low average densities ρ_o, the spatially constant 'liquid' solution dominates. As the density increases, a periodic, 'crystalline' solution appears. What is interesting from the glassy point of view, is that in the high density regime, there appear also many non-periodic 'amorphous' solutions. Each one of these is supposed to represent a metastable glassy state. These states are local minima of (1) satisfying (2). Beyond the mean-field approximation, high free-energy solutions are unstabilized by nucleation; if we wish to model the realistic situation we should look for the solutions that are deepest in free energy—excluding, of course, the crystalline state. We have then a situation analogous to the one described above for chaotic systems: of all the solutions satisfying the "equations of motion" (2), we have to look for the configurations that minimize globally free energy (1), and ask whether these "large deviation" solutions have special regularity properties.

This analogy between dynamical systems that are chaotic in time, and glassy systems that are chaotic in space, was pointed out many years ago by Ruelle [5]. It has also appeared in the theory of charge-density waves [6–8], in particular in the Frenkel-Kontorova model. It turns out that the local energy minima of the model are given by the trajectories of the "standard map", which has both regular and chaotic orbits. However, when one restricts to the lowest energy minima, the trajectories selected are quasiperiodic.

In a recent paper it was argued [9] that ideal glasses should exhibit a form of geometrical order that is more general than periodic and quasiperiodic, characterized by the fact that local motifs of all sizes are repeated often. For a system that is not completely ordered, this assumption leads to the definition of a correlation length, defined as the largest size of patterns that repeat more frequently than they would in a random case. The claim is then that this correlation length should diverge in an ideal glass. But frequent repetitions of patterns would not occur for a generic solution of a spatially chaotic glass. If order in the solution is to happen at all it is through a mechanism as described above: choosing configurations that globally minimize energy would then force the system to favor some patterns that would consequently be repeated often.

In the present work we treat a simple example. The system studied has the advantage that it is purely chaotic, we know that there are no islands of regular dynamics in phase-space. If the large-deviation bias selects orbits which have some regularity, it does so in the most unfavorable situation in which these orbits are isolated and unstable. The organization of this paper is as follows: In Sect. 2, we present the baker's map and the functional used in our model. In Sect. 3, the trajectories that extremize the functional are found and their order properties are discussed.

2 The Model

In this section we briefly review the baker's map and some of its properties. We then define the functional used in our model and whose minimal trajectories will be studied later.

2.1 The Baker's Map

The baker's map is a simple two-dimensional chaotic map acting on the unit square. The dynamical system with discretized time t, associated with the baker's map, is defined for $q_t \in [0, 1]$ and $p_t \in [0, 1]$ by the area-preserving equations

$$q_{t+1} = 2q_t - \lfloor 2q_t \rfloor \tag{3}$$

$$p_{t+1} = \frac{1}{2}(p_t + \lfloor 2q_t \rfloor) \tag{4}$$

where $\lfloor 2q_t \rfloor$ is the integer part of $2q_t$. As shown by Fig. 1, the phase square is stretched in the q direction and squeezed it in the p direction; the baker then cuts the right part and puts it on top of the left one.

The baker's map can also be understood as a shift operator. Let us consider the binary representations $q_t = 0.abc\ldots$ and $p_t = 0.uvw\ldots$ where a, b, c, u, v, w, $\ldots$ are either 0 or 1. If the position (q_t, p_t) of the system at time t is written as the string "$\ldots wvu \cdot abc\ldots$", the state of system at time $t + 1$ is obtained by shifting the central dot to the right by one position, that is, the string becomes "$\ldots wvua \cdot bc\ldots$" and we have $q_t = 0.bcd\ldots$ and $p_t = 0.auv\ldots$.

The baker's map is deterministic: if the system is started at initial conditions (q_0, p_0), (3) and (4) determine its position at all future (and past) times. However, the system is chaotic in the sense that a small uncertainty in the initial conditions grows exponentially in time (the shift operator doubles it at each iteration); when the uncertainty reaches the size of the phase square (here, this size is unity), the position of the system becomes unpredictable.

Although almost all trajectories are aperiodic, there are many initial conditions leading to periodic orbits. Considering the shift operator interpretation and remembering that the binary representation of a rational number has a periodic pattern, one sees that the periodic orbits are related to rational numbers. In Fig. 2 (left), the rational number 5/31 (whose binary representation is the periodic string $0.00101\,00101\,00101\ldots$) was chosen as the initial position q_0 (the top-left point). The ordinate p_0 is such that its binary representation is the mirror of q_0's binary representation. After five units of time, the dot shifts five times to the right and one has $q_5 = q_0$; thus, the orbit is periodic with period 5. A periodic orbit can be described by the binary digits of the periodic pattern in the binary representation. In our example, the orbit is $\{n_4, \ldots, n_0\} = \{0, 0, 1, 0, 1\}$. Obviously, a cyclic permutation of these five digits doesn't change the orbit.
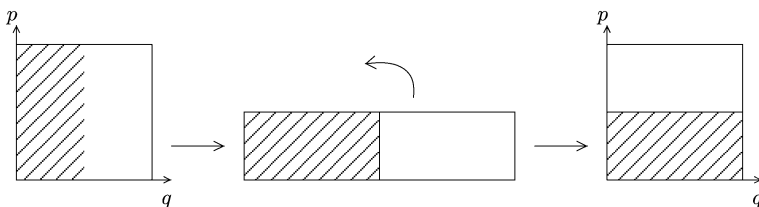
Fig. 1 One iteration of the baker's map
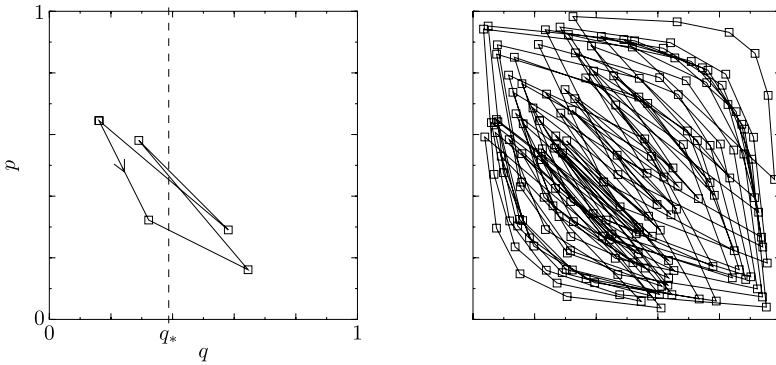
Fig. 2 Representation of the periodic orbit $\{n_4, \ldots, n_0\} = \{0, 0, 1, 0, 1\}$ in the phase square (*left*). The arrow shows the direction of the trajectory. An irregular orbit that never is an extremal trajectory, for any q_* (*right*)

Strictly speaking, the binary representation of a rational is not always periodic, but the non-periodic part is located near the dot and has a finite length. For example, the number $q_0 = 5/31 + 1/4$ is written as $0.011\,01001\,01001\ldots$. After many iterations of the map, the system forgets the 1/4 term in q_0 (its second most significant bit), because it is shifted to less and less significant places in the binary representation of p_t; the initial p_0 is forgotten as well. It is clear that as long as the initial position q_0 is rational, the trajectory falls into a periodic orbit after some time. If a q_0 is chosen randomly and uniformly in the unit interval, it is irrational. Indeed, although rational numbers are dense in the unit interval, they form a set with zero measure. As a consequence, typical trajectories are not periodic. Because the baker's map is ergodic, such a typical trajectory fills up uniformly the phase square. Furthermore, a small perturbation of an initial condition associated with a periodic orbit yields a chaotic orbit.

The baker's map has two unstable fixed points which correspond to periodic orbits with period one. These two orbits are $\{0\}$ and $\{1\}$, respectively the points located at the origin $(0, 0)$ and the opposite corner $(1, 1)$.

2.2 Large Deviations

Let us introduce in our model an observable which is a functional of the trajectories. Our choice is arbitrary, we are motivated here by simplicity. We consider a functional parametrized by a number q_* in $[0, 1]$:

$$h[\{q_t\}, q_*] = \lim_{T \to \infty} \frac{1}{T} \sum_{t=0}^{T-1} (q_t - q_*)^2 \tag{5}$$

The observable h can be interpreted geometrically as the average squared distance over time between the trajectory and a reference vertical line located at q_*, as schematically represented in Fig. 2. For each value of the parameter q_*, there is one particular trajectory that minimizes the average distance h. Note that h is invariant by the transformation $(q_t, q_*) \to (1 - q_t, 1 - q_*)$ so if $\{q_t\}$ is an extremal trajectory for $q_* \leq \frac{1}{2}$, $\{1 - q_t\}$ is an extremal trajectory for $1 - q_* \geq \frac{1}{2}$. Hence, we can restrict the study to $0 \leq q_* \leq \frac{1}{2}$. Although the baker's map is bidimensional, the problem is actually one-dimensional only, because the dynamics on the q axis are not coupled to the one on the p axis, as shown by (3). The

Fig. 3 Value of the observable (5) for the minimal trajectory (*lowest curve*), the maximal trajectory (*highest curve*) and a typical trajectory (*middle curve*)
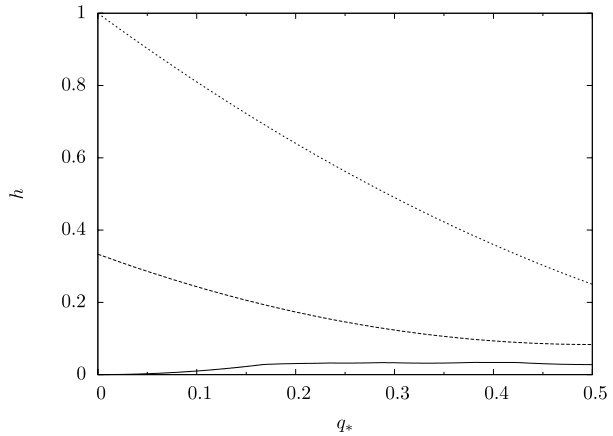
two-dimensional generalization of the observable (5) would be the average squared distance between the trajectory and a reference *point* located at (q_*, p_*):

$$\lim_{T \to \infty} \frac{1}{T} \sum_{t=0}^{T-1} [(q_t - q_*)^2 + (p_t - p_*)^2] \qquad (6)$$

The extremal trajectories for (q_*, p_*) of the observable (6) are easily deduced from the extremal trajectories of the one-dimensional observable (5) for the parameter $\frac{1}{2}(q_* + p_*)$. It will indeed be clear later that the extremal trajectories are left invariant by the transformation that swaps the q and p axis; this transformation is equivalent to reversing the time. The orbit in Fig. 2 is for example the minimal trajectory for the chosen value of q_* (and actually for any q_* in the whole range $[0.385, 0.411]$) and has the $(p \leftrightarrow q)$ symmetry, as do the orbits of Fig. 6.

The worse state in the sense of minimization of h is one of the two fixed points. If $q_* \leq \frac{1}{2}$, this maximal trajectory is the fixed point $(1, 1)$ and we have $h = (1 - q_*)^2$. On the other hand, the distribution of the q_t for a chaotic trajectory is uniform in the unit interval and the mean distance is calculated by the continuous sum

$$h_{\text{chaotic}}(q_*) = \int_0^1 (q - q_*)^2 \, dq = \frac{1}{3} - q_*(1 - q_*) \qquad (7)$$

Figure 3 shows the energies of the minimal orbit (which we shall determine below), the maximal orbit and a typical (i.e. chaotic) orbit. It is worth noting that chaotic orbits never minimize or maximize the functional. In the next sections, the minimal trajectories of h are made explicit and found to be periodic for most values of q_* and quasi-periodic for some (zero measure) set of values of q_*.

3 Large-Deviation Function as a Free Energy of a 1D Lattice Gas Model

3.1 Mapping to the Particle Model

In this section, we will show that the functional (5) can be interpreted as the Hamiltonian of particles on a one-dimensional lattice with single occupancy and a translationally invariant

interaction. That is,

$$h = \frac{1}{M} \sum_{i,j=1}^{M} U_{|i-j|} n_i n_j - \mu\rho + h_0$$

where ρ is the particle density, and μ acts as a chemical potential. The interaction will be shown to decay exponentially with distance.

As stated earlier, a point on a periodic orbit (of period N) is represented by the binary sequence $0.n_{N-1} \ldots n_1 n_0 n_{N-1} \ldots \equiv \{n_{N-1}, \ldots, n_1, n_0\}$. Note that this number may be written as

$$\{n_{N-1}, \ldots, n_0\} = \frac{1}{2^N - 1}(2^{N-1} n_{N-1} + \cdots + 2^1 n_1 + n_0)$$

We define σ as the cyclic left shift operator (or left cyclic permutation) to be applied on the digits n_i of the period, that is

$$\sigma\{n_{N-1}, \ldots, n_1, n_0\} = \{n_{N-2}, \ldots, n_0, n_{N-1}\}$$

The ith iteration of σ may be written as

$$\sigma^i\{n_{N-1}, \ldots, n_0\} = \frac{1}{2^N - 1} \sum_{j=0}^{N-1} 2^{[j+i]} n_j$$

Here and in what follows [•] denotes the exponents and indices modulo N.

Taking into account the periodicity and expanding, the observable (5) now reads

$$h = u - \mu\rho + h_0 \tag{8}$$

where

$$\rho = \frac{1}{N} \sum_{j=0}^{N-1} n_j, \qquad \mu = 2q_*, \qquad h_0 = q_*^2 \tag{9}$$

and with u given by

$$u = \frac{1}{N} \sum (\sigma^i\{n_{N-1}, \ldots, n_0\})^2 = \frac{1}{N(2^N - 1)^2} \sum_i \sum_{jk} 2^{[j+i]} 2^{[k+i]} n_j n_k$$

$$= \frac{1}{N} \sum_{jr} \left(\frac{1}{(2^N - 1)^2} \sum_i 2^{[j+i]} 2^{[j+r+i]} \right) n_j n_{[j+r]} \tag{10}$$

In the above, all the indices are summed from 0 to $N - 1$. Shifting the exponents on the right hand side as $i \to [i - j]$ we get:

$$u = \frac{1}{N} \sum_{jr} U_r^{(N)} n_j n_{[j+r]} \quad \text{with } U_r^{(N)} = \frac{1}{(2^N - 1)^2} \sum_i 2^{[i]} 2^{[r+i]} \tag{11}$$

In Appendix A we show that

$$U_r^{(N)} = \frac{1}{3} \frac{2^{N-r} + 2^r}{2^N - 1} \tag{12}$$

3.2 The Long-Orbit Limit

Consider now a very long chain of size M, particles with occupation numbers n_i, and an interaction given by

$$h = \frac{1}{M} \sum_{i,j=1}^{M} U_{|i-j|} n_i n_j - \frac{\mu}{M} \sum_{i=1}^{M} n_i + h_0 = \frac{1}{3M} \sum_{i,j=1}^{M} 2^{-|i-j|} n_i n_j - 2q_*\rho + (q_*)^2 \quad (13)$$

that is, $U_r = \frac{1}{3} 2^{-|r|}$. Let us compute the energy of a periodic configuration of period $N \ll M$. We can re-express the unrestricted sum (13) as a sum over the first period as in Fig. 4, adding first each position r within the first period with its repetitions in all other periods. We may express these contributions as two geometric series, corresponding to the particles to the right and to the left, respectively:

$$\frac{1}{3}\{[2^{-r} + 2^{-(N+r)} + 2^{-(2N+r)} + \cdots] + [2^{-(N-r)} + 2^{-(2N-r)} + 2^{-(3N-r)} + \cdots]\}$$

$$= \frac{1}{3} \frac{1}{(1-2^{-N})} [2^{-r} + 2^{-N+r}] = \frac{1}{3} \frac{2^{N-r} + 2^r}{2^N - 1} = U_r^{(N)} \quad (14)$$

Thus, (11) is recovered. This means that we may consider, without loss of generality, a very long periodic chain of size M, and the energy of periodic configurations of periods $N \ll M$ will be correctly computed by the interaction (13). This, in turn means that our large functional (5) can be computed for large times on the basis of the particle model (13).

3.3 Large Deviation Function

Given a time T, we express the probability of observing a value of the quantity defined in (5) as:

$$P(h[q_t, q_*] = h) = e^{-T\xi(h)} \quad (15)$$

Fig. 4 Counting the energy of a periodic configuration as the sum of two geometric series, corresponding to the set of periods to the *right*, and to the *left*, respectively

N

r , N+r, N+2r, ...

N−r, 2N−r, 3N−r, ...
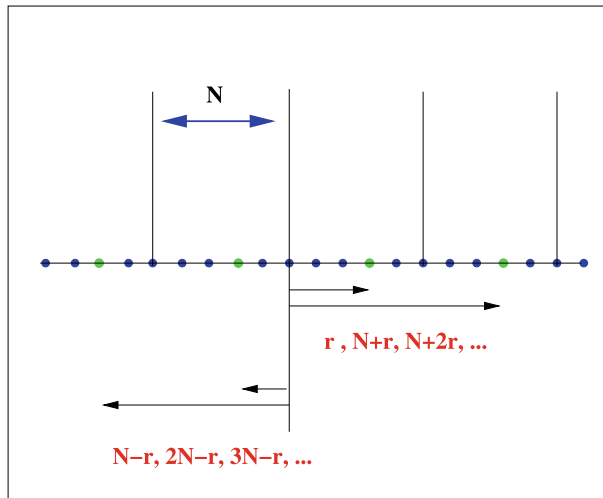
this defines $\xi(h)$. Alternatively, we may express the same information in the large deviation function $f(\lambda)$:

$$e^{-Tf(\lambda)} = \int d\lambda\, P(h[q_t, q_*] = h)e^{-\lambda Th} \tag{16}$$

For long times T, we have that ξ and f are related by a Legendre transform. In fact, we recognize $f(\lambda)$ as the free energy density of the particle model at inverse temperature λ. In particular, the ground state (corresponding to infinite λ) is given by the trajectory minimizing h.

3.4 The Ground State of the Lattice Particle Model

Let us start by considering the minimum of the energy (13) :

$$\min\{h\} = \min\left\{\frac{1}{M}\sum_{jr} U_r n_j n_{[j+r]} - 2q_*\rho + (q_*)^2\right\} = \min_{\rho}\{U^{\min}(\rho) - 2q_*\rho + (q_*)^2\} \tag{17}$$

where $U^{\min}(\rho)$ is the smallest energy for a fixed configuration density. Although it is tempting to determine the value of ρ of the extremal configuration by

$$\frac{dU^{\min}(\rho)}{d\rho} = 2q_* \tag{18}$$

this must be treated with care, because as we shall see, the derivative is discontinuous. Note again that q_* plays the role of a chemical potential.

Our job is now to determine $U^{\min}(\rho)$. This problem was solved years ago [10, 11] for long-range ($U_r > 0\ \forall r$) interactions with U_r convex downwards, as is the case here.

For the moment, let us forget the lattice. If the particles can take any position on a one-dimensional line with periodic boundary conditions, the ground state is simply a crystal, that is, each particle is separated from its neighbor by the same distance $d = 1/\rho$. The condition of convexity of the interactions can be understood as a stability condition. Indeed, if one considers a first-neighbor concave interaction as shown in Fig. 5 (left), a displacement of one particle in the crystal would decrease the energy of the system: the system is not stable. On the contrary, if the first-neighbor interaction is convex as shown in Fig. 5 (right), a displacement of one particle would increase the energy of the system.

For particles constrained to lie on a lattice, if ρ is such that the mean distance $1/\rho$ is an integer, then the ground state is again periodic with particles separated by this same distance

Fig. 5 Change Δu of the energy of a crystal configuration after the displacement of one particle for a concave interaction (*left*) and a convex interaction (*right*)
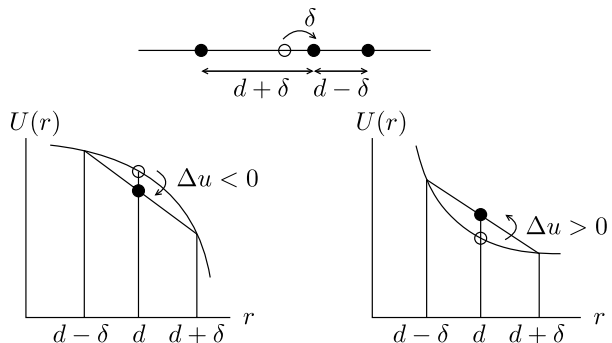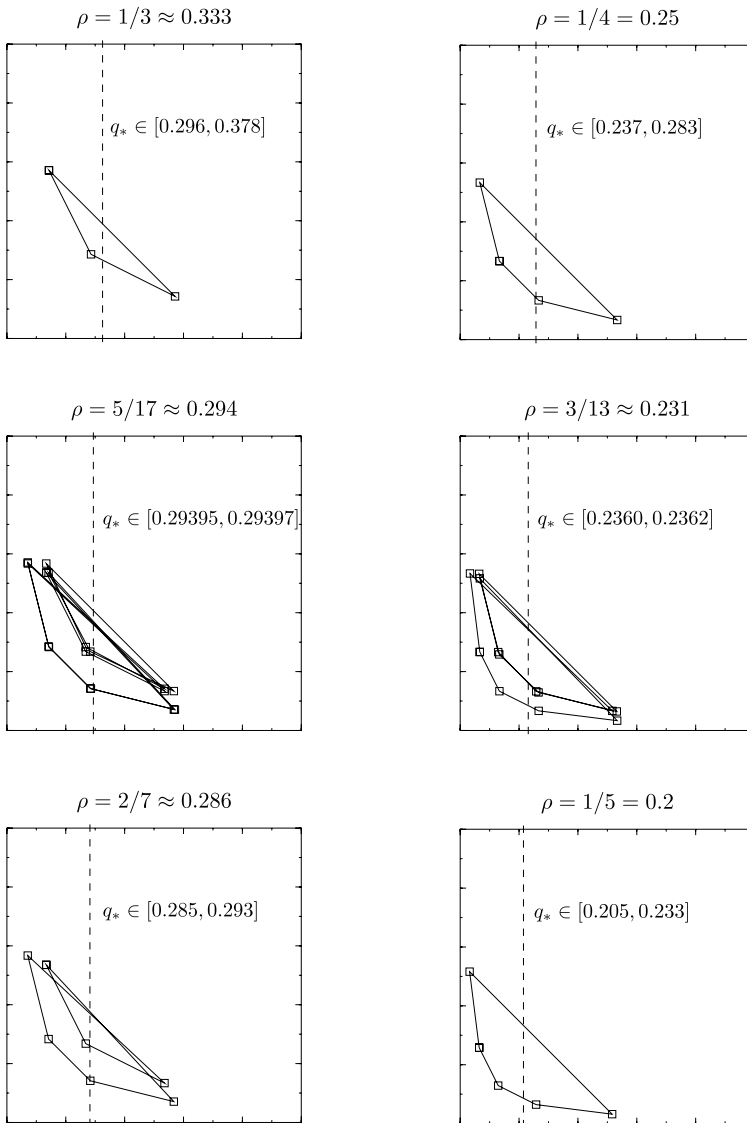
Fig. 6 Examples of minimal orbits for different values of q_*. The density of 1's ρ of the orbits are indicated

$1/\rho$. In the baker's map representation, the trajectory corresponding to such a crystal is very regular. Figure 6 shows the $\rho = \frac{1}{3}$, $\rho = \frac{1}{4}$ and $\rho = \frac{1}{5}$ minimal trajectories. As $1/\rho$ becomes larger, the minimal trajectory spends more and more time near the fixed point $(0, 0)$.

If $1/\rho$ is not an integer, then it lies between the two successive integers $d = \lfloor 1/\rho \rfloor$ and $d + 1$, and the distance between any two consecutive particles will be either d or $d + 1$. There is a competition between the solution with density $1/d$ and the one with density $1/(d + 1)$. This is seen in the baker's map, where Fig. 6 shows that the trajectory for $\rho = 5/17$ spends some time in the $\rho = 1/4$ (period 4) solution and some time in the $\rho = 1/3$ (period 3)

Fig. 7 The period of the minimal trajectory as a function of q_*. The fractions specify the density ρ of particles in the corresponding configuration. Only the largest steps are indicated
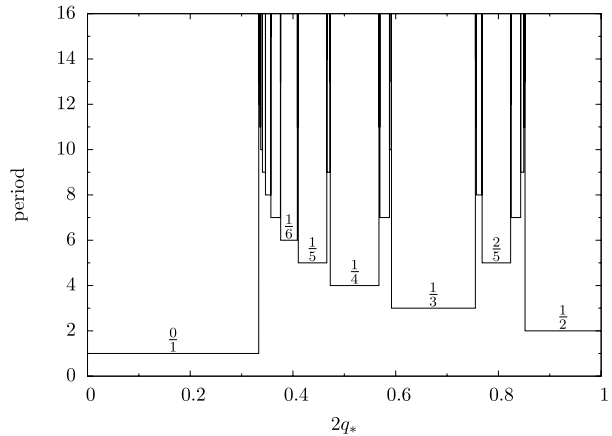
Fig. 8 Determination of the ground state of the lattice Hamiltonian for $\rho = 3/7$. The arrows indicate the position of the particles
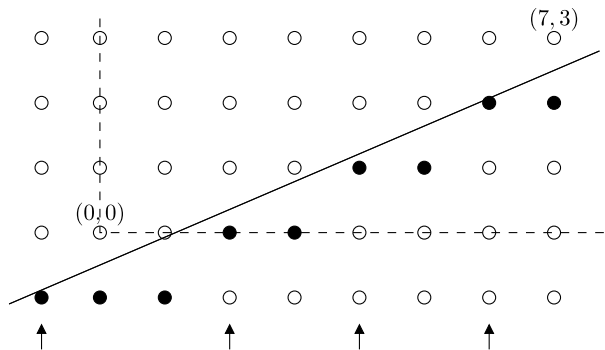
solution. The competition between the two solutions $1/d$ and $1/(d + 1)$ is also seen in Fig. 7. In this figure, the $1/d$ solutions are seen to dominate for some large range of values of q_*. When varying the parameter q_* continuously in order to go from the $1/d$ solution to the $1/(d + 1)$ solution, the period takes many intermediate values "interpolating" between periods 3 and 4.

Let us now turn to the full solution, which was originally given in terms of continued fractions [10, 11] and admits a graphical construction related to that employed in quasicrystals [12, 13] which we will describe. Consider the plane and the lattice of points with integer coordinates, as shown in Fig. 8, and the line with slope ρ starting at the origin $(0, 0)$. The algorithm to solve the problem is quite simple: for each integer abscissa k, compute the ideal ordinate $k\rho$ and round it to the closest smaller integer y_k, then, mark the point (k, y_k). The ground state corresponding to density ρ is simply given by the sequence of binary digits $n_k = y_k - y_{k-1}$, that is, there is a particle in site k in places where the black pixels have a step upwards. In fact, the line can start at any arbitrary point; this leads to different sequences with the same energy. These sequences have the form

$$n_k = \lfloor k\rho + \phi \rfloor - \lfloor (k - 1)\rho + \phi \rfloor \tag{19}$$

where ϕ is a phase factor related to the y-intercept of the line. Figure 8 shows the determination of the ground state for $\rho = 3/7$. One can read directly the ground state by looking at the ordinates of the black pixels.

Following Aubry [14], one can obtain an exact expression for the energy $U^{\min}(\rho)$. We need to introduce first another useful representation of the ground state. If x_j is the position the jth particle, we have

$$x_j = \left\lfloor \frac{j}{\rho} + \text{const} \right\rfloor \tag{20}$$

Next, we rewrite the interaction term as

$$U = \sum_r u_r \tag{21}$$

where the u_r is the average contribution of all pairs of rth neighboring particles

$$u_r = \rho \langle U(x_{j+r} - x_j) \rangle \tag{22}$$

and $\langle \bullet \rangle$ denotes averaging over all such pairs, in the limit $M \to \infty$. Let us derive an explicit expression for the u_r. The distance $x_{j+r} - x_j$ between two particles separated by $r-1$ others, is either $\lfloor r\rho^{-1} \rfloor$ or $\lfloor r\rho^{-1} \rfloor + 1$. If π_r is the fraction of pairs having the value $\lfloor r\rho^{-1} \rfloor$, and $(1 - \pi_r)$ of having $\lfloor r\rho^{-1} \rfloor + 1$, $\langle x_{j+r} - x_j \rangle$ is by definition $\pi_r \lfloor r\rho^{-1} \rfloor + (1 - \pi_r)(\lfloor r\rho^{-1} \rfloor + 1)$. Using the fact that

$$\langle x_{j+r} - x_j \rangle = \langle x_{j+r} - (j+r)\rho^{-1} \rangle - \langle x_j - j\rho^{-1} \rangle + r\rho^{-1} = r\rho^{-1}$$

we conclude that

$$\pi_r = 1 - (r\rho^{-1} - \lfloor r\rho^{-1} \rfloor)$$

We thus obtain an explicit expression of the interaction term:

$$U^{\min} = \rho \sum_r [\pi_r U(\lfloor r\rho^{-1} \rfloor) + (1 - \pi_r) U(\lfloor r\rho^{-1} \rfloor + 1)]$$

$$= \frac{1}{2} \sum_r (2 - (r\rho^{-1} - \lfloor r\rho^{-1} \rfloor))\rho U(\lfloor r\rho^{-1} \rfloor) \tag{23}$$

$U^{\min}$ is continuous everywhere and its derivative

$$u'(\rho) = \frac{dU^{\min}}{d\rho} = \sum_r \left(1 + \frac{1}{2}\lfloor r\rho^{-1} \rfloor\right) U(\lfloor r\rho^{-1} \rfloor) \tag{24}$$

is an increasing function, as shown in Fig. 9.

The density can be determined from the knowledge of q_* following (18): the y-axis in Fig. 9 is $2q_*$. When the level $2q_*$ hits on an interval between two values, the lower step is chosen. The density ρ is thus given by Fig. 10. Once ρ is known, the configuration can be obtained either graphically from Fig. 8, or with (20). The value of the 'energy' can be obtained from (17) and (23), or the top part of Fig. 9.

If $2q_*$ falls between two steps of the $u'(\rho)$ curve, i.e. there exists a ρ such that $u'(\rho^-) \leq \mu \leq u'(\rho^+)$, then ρ is rational and is the density of the ground state; the configuration of particles is consequently periodic. The width of the interval of q_* corresponding to this density is given by the discontinuity of the energy's slope $2\delta q_*(\rho) = u'(\rho^+) - u'(\rho^-)$ If, on the contrary, there exists a ρ such that $u'(\rho) = 2q_*$, then ρ is irrational: the ground state has density ρ and the configuration of particles is quasi-periodic.

Fig. 9 Energy $u = h(q_* = 0)$ and its first derivative $du/d\rho$ plotted versus the density ρ
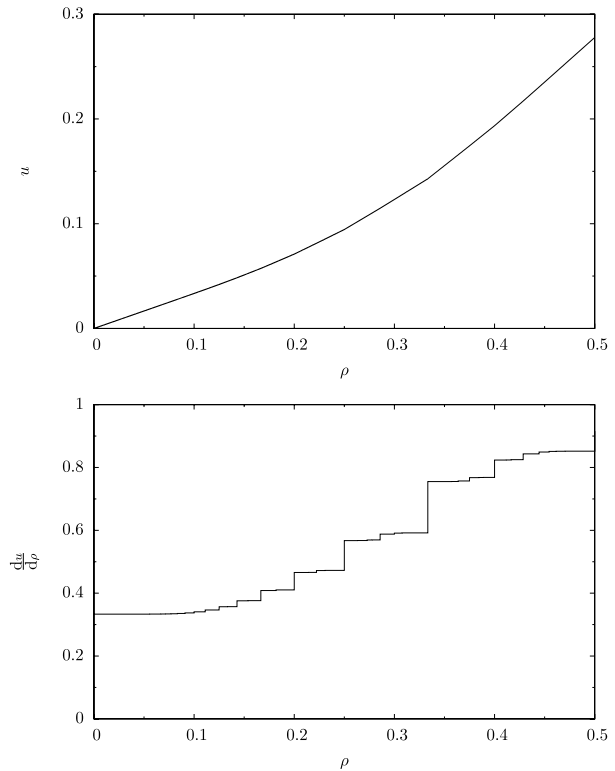
There exists a smallest integer r such that $r\rho^{-1} = s$ where s is an integer. For this r and for all its multiples kr, $u'_{kr}(\rho)$ is discontinuous and $\sum_{k,r}(u'_{kr}(\rho^+) - u'_{kr}(\rho^-))$ is the sum of the discontinuities. We obtain, with $\rho = \frac{r}{s}$

$$(u'(\rho^+) - u'(\rho^-)) = \frac{1}{3}\sum_{k=1}^{\infty}(ks)2^{-ks} = \frac{s}{3}\frac{2^s}{(2^s-1)^2}$$

Note that the result does not depend on the numerator r.

Although a quasi-periodic ground state can be obtained by choosing the right q_*, the set of such particular values has zero measure. Indeed, the sum of all discontinuities of $u'(\rho)$ for $0 \le \rho \le 1$ rational, is

$$\Delta = \sum_{\rho = \frac{r}{s} \in [0,1]}(u'(\rho^+) - u'(\rho^-)) = \frac{1}{3}\sum_{s=1}^{\infty}\sum_{k=1}^{\infty}\varphi(s)(ks)2^{-ks}$$

where $\varphi(s)$ is the Euler function equal to the number of integers in $[1, s-1]$ that are coprime to s. Using the change of variable $u = ks$ and a known property of the Euler function, we obtain

$$\Delta = \frac{1}{3}\sum_{u=1}^{\infty}u2^{-u}\sum_{k|u}\varphi(k) = \frac{1}{3}\sum_{u=1}^{\infty}u^2 2^{-u} = \frac{4}{3}$$

Fig. 10 The density ρ of the ground state plotted versus the chemical potential $\mu = 2q_*$. This curve is a complete devil's staircase
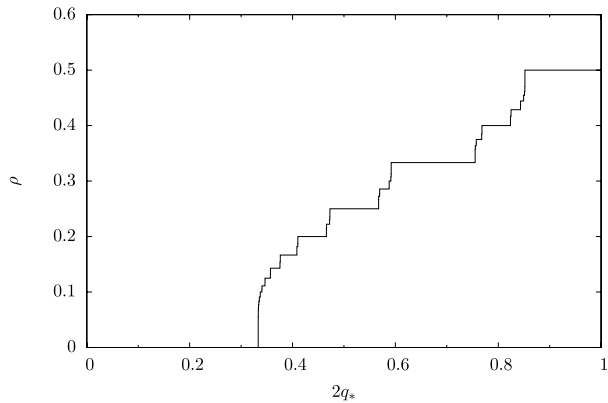
We have proved that $\Delta = \frac{4}{3} = u'(1) - u'(0)$, that is, the probability that a fixed q_* falls between steps is one. In other words, the probability that the density is rational is one and the set of values of q_* associated with quasi-periodic orbits has zero measure.

The solution $\rho(q_*)$ plotted in Fig. 10 has a devil's staircase structure: it is a *continuous* curve, constant on some interval when ρ is rational.

4 Concluding Remarks

We have studied the trajectories of the baker's map that extremize the average squared distance to a line $q = q_*$. The minimal trajectory is periodic for most values of q_*; and quasi-periodic for a zero-measure set of values of q_*. For all values of q_*, the minimal trajectory exhibits more order than the generic chaotic trajectories. This does not mean that the trajectories involved are not chaotic in the sense of being insensitive to boundary conditions: a slight perturbation of the initial condition of an extremal trajectory leads to a new trajectory that departs away from the periodic one, and ultimately explores ergodically all phase-space—thus spoiling its extremal properties.

The ordered structure of the minimizing state highly depends on fact that the corresponding Hamiltonian in the 1D lattice gas has infinite range. In the case in which the Hamiltonian of the 1D lattice gas has a finite range ($U_r = 0$ for $r > R$—one may think about a hard-sphere model), for small enough density any configuration with interparticle distance $> R$ minimizes the energy; and the vast majority of configurations is not ordered. This is easy to understand for the baker's map: such an interaction corresponds to minimizing a functional that does not depend on all digits of the positions, i.e. it is a functional in which the trajectories contribute in a degenerate manner.

In the other extreme, functionals that are long-range in time may also yield disordered extremal trajectories. For the baker's map, the observable to be minimized could be

$$\lim_{T\to\infty}\left(\frac{1}{T}\sum_{t=0}^{T-1}(\lfloor 2q_t\rfloor - 1/2)\right)^2$$

where $\lfloor 2q_t\rfloor$ is the tth binary digit of q_0. This is a long-range antiferromagnet: the sum thus has disordered, degenerate ground states. Note that this observable is not local in the sense that the position at time t is coupled to the position at different time t'.

In conclusion, we have presented a simple example illustrating that those trajectories of a map which extremize some functional may exhibit structure absent in the entire ensemble of trajectories. This is reminiscent of the Frenkel-Kontorova model, where the ground states possess quasiperiodic translational order [6–8], while other stationary solutions do not. It is tempting to conjecture that such behavior is the rule rather than the exception, and may therefore be relevant to systems which are chaotic in either the spatial or temporal domain.

Appendix A

Let us start with

$$U_r^{(N)} = \frac{1}{(2^N - 1)^2} \sum_i 2^i 2^{i+r} \tag{25}$$

We first determine $U_0^{(N)}$:

$$U_0 = \frac{1}{3} \frac{2^N + 1}{2^N - 1} \tag{26}$$

Next, let us express $U_{r+1}^{(N)}$ in terms of $U_r^{(N)}$. We split the sums in

$$U_{r+1} = \frac{1}{(2^N - 1)^2} \sum_{i=0}^{N-1} 2^i 2^{[i+r+1]} \tag{27}$$

as

$$\sum_{i=0}^{N-1} = \sum_{i+r+1<N} + \sum_{i+r+1\geq N} = \sum_{i=0}^{N-r-2} + \sum_{i=N-r-1}^{N-1} \tag{28}$$

so that

$$U_{r+1}^{(N)} = \frac{1}{(2^N - 1)^2} \left(\sum_{i=0}^{N-r-2} 2^i 2^{i+r+1} + \sum_{i=N-r-1}^{N-1} 2^i 2^{i+r+1-N} \right) \tag{29}$$

(here the exponents are not necessarily modulo N). The first and second sums read:

$$\sum_{i=0}^{N-r-2} 2^i 2^{i+r+1} = 2 \left(\sum_{i=0}^{N-r-1} 2^i 2^{i+r+1} \right) - 2^{N-r-1} 2^N \tag{30}$$

and

$$\sum_{i=N-r-1}^{N-1} 2^i 2^{i+r+1-N} = 2 \left(\sum_{i=N-r}^{N-1} 2^i 2^{i+r-N} \right) + 2^{N-r-1} \tag{31}$$

so that (29) can be written

$$U_{r+1}^{(N)} = 2U_r^{(N)} - \frac{1}{(2^N - 1)^2} (2^{N-r-1} 2^N - 2^{N-r-1}) \tag{32}$$

$$U_{r+1}^{(N)} = 2U_r^{(N)} - \frac{2^{N-r-1}}{2^N - 1} \tag{33}$$

or:

$$\left(2^{r+1} U_{r+1}^{(N)}\right) = 4\left(2^r U_r^{(N)}\right) - C \tag{34}$$

with $C = 1/(1 - 2^{-N})$. Putting

$$b_r = 2^r U_r^{(N)} - \frac{C}{3} \tag{35}$$

the recurrence equation becomes

$$b_{r+1} = 4b_r \tag{36}$$

which implies that $b_r = b_0 4^r$, with $b_0 = U_0^{(N)} - \frac{C}{3}$, leading to:

$$U_r^{(N)} = \frac{C}{3} + 4^r \left(U_0^{(N)} - \frac{C}{3}\right) = \frac{1}{3}\frac{2^{N-r} + 2^r}{2^N - 1} \tag{37}$$

References

1. Singh, Y., Stoessel, J.P., Wolynes, P.G.: Phys. Rev. Lett. **54**, 1059 (1985)
2. Dasgupta, C.: Europhys. Lett. **20**, 131 (1992)
3. Dasgupta, C., Ramaswamy, S.: Physica A **186**, 314 (1992)
4. Ramakrishnan, T.V., Yussouff, M.: Phys. Rev. B **19**, 2775 (1979)
5. Ruelle, D.: Physica A **113**, 619 (1982)
6. Aubry, S.: Physica D **7**, 240 (1983)
7. Aubry, S.: J. Phys. **44**, 147 (1983)
8. Coppersmith, S.N., Fisher, D.S.: Phys. Rev. B **28**, 2566 (1983)
9. Kurchan, J., Levine, D.: Correlation length for amorphous systems, arXiv:0904.4850
10. Hubbard, J.: Phys. Rev. B **17**, 494 (1978)
11. Pokrovsky, V.L., Uimin, G.V.: J. Phys. C **11**, 3535 (1978)
12. de Bruijn, N.G.: Kon. Nederl. Akad. Wetensch. Proc. Ser. A (1981)
13. Steinhardt, P.J., Ostlund, S.: The Physics of Quasicrystals. World Scientific, Singapore (1987) (Chap. 1)
14. Aubry, S.: J. Phys. C Solid State Phys. **16**, 2497 (1983)